NASA
Technical Memorandum 4313

AVSCOM
Technical Report 91-B-017

An Experimental Study of the Sensitivity of Helicopter Rotor Blade Tracking to Root Pitch Adjustment in Hover

W. Keats Wilkie, Chester W. Langston,
Paul H. Mirick, Jeffrey D. Singleton,
Matthew L. Wilbur, and William T. Yeager, Jr.
Aerostructures Directorate
U.S. Army-AVSCOM
Langley Research Center
Hampton, Virginia

National Aeronautics and
Space Administration

Office of Management

Scientific and Technical
Information Program

1991

Summary

The sensitivity of blade tracking in hover to variations in root pitch was examined for two rotor configurations. Tests were conducted using a four-bladed articulated rotor mounted on the NASA/U.S. Army aeroelastic rotor experimental system (ARES) at the Langley Research Center. Two rotor configurations were tested: one consisting of a blade set with flexible fiberglass spars and one with stiffer (by a factor of five in flapwise and torsional stiffnesses) aluminum spars. Both blade sets were identical in planform and airfoil distribution and were untwisted. The two configurations were ballasted to the same Lock number so that a direct comparison of the tracking sensitivity to a gross change in blade stiffness could be made.

Experimental results show no large differences between the two sets of blades in the sensitivity of the blade tracking to root pitch adjustments. However, a measurable reduction in in-track coning of the fiberglass spar blades with respect to the aluminum blades is noted at higher rotor thrust conditions.

Introduction

A major concern in developing any new rotor design is the relative sensitivity of that design to track adjustment (or misadjustment). An out-of-track blade can often cause unacceptable once-per-revolution vibrations on a helicopter, and correcting such a track problem can be a laborious and time-consuming process. Usual methods employed to correct a track problem involve adjusting blade root pitch, deflecting trailing edge tabs, or adding balance weights to lower the once-per-revolution vibrations caused by the errant blade to acceptable levels. Such methods are for the most part trial-and-error in nature and unresponsive blades often must be discarded altogether. Past studies (refs. 1 and 2) have suggested that torsionally "soft" rotor blades are especially sensitive to parametric track adjustments. The rather large sensitivity, and relatively unpredictable tracking response, of such blades to small tracking adjustments was recognized as a potential problem for full-scale rotors. As a first step to understanding out-of-track blade phenomena, this study attempts to experimentally quantify the tracking sensitivities in hover of two rotor configurations with comparatively large differences in blade structural stiffness. The results presented in this paper address only tracking response due to discrete changes in root pitch, and only for an articulated rotor.

Symbols

a	blade section two-dimensional lift-curve slope, per radian
b	number of blades
c	blade chord, ft
C_T	rotor thrust coefficient, $T \Big/ \left[\rho\pi R^2(\Omega R)^2\right]$
I_b	rotor blade flapping mass moment of inertia about flapping axis, slug-ft^2
I_θ	rotor blade torsional mass moment of inertia, per unit length about blade elastic axis, lb-sec^2
R	rotor radius, ft
r	spanwise distance along blade radius measured from center of rotation, ft
T	rotor thrust force, measured from balance normal-force channel, lb
β	blade coning angle, deg
$\Delta\beta$	induced blade out-of-track with respect to reference blade, deg
γ	blade Lock number, $c\rho a R^4/I_b$
θ	rotor blade collective pitch angle, deg
$\Delta\theta$	offset increment of root pitch applied to perturb blade, deg
ρ	mass density of test medium, slug/ft^3
σ	rotor solidity, $bc/\pi R$
Ω	rotor rotational velocity, rad/sec
ω	natural frequency of rotating blade mode, rad/sec

Apparatus and Procedures

Test Facility

Testing was conducted in the Langley Helicopter Hover Facility (HHF), shown in figure 1. The HHF is a high-bay facility enclosed by a 30-ft × 30-ft × 20-ft coarse-mesh screen and is used for hover testing and rotorcraft model buildup and checkout prior to testing in the Langley Transonic Dynamics Tunnel (TDT). Models are mounted on the test stand such that the rotor plane of rotation is high enough above the floor to avoid ground effect (15 ft, or approximately 1.6 times the rotor diameter). All hover testing in the HHF is performed at sea level atmospheric conditions (nominal $\rho = 0.002378$ slug/ft^3).

Model Description

A four-bladed articulated hub with coincident lead-lag and flapping hinges was used in this investigation. Two sets of rotor blades were used: one set

with flexible fiberglass spars and one set with stiffer aluminum spars. The structural and inertial properties of both blade sets are listed in tables I and II. Rotating natural frequencies were computed using the Comprehensive Analytical Model of Rotorcraft Aerodynamics and Dynamics (CAMRAD) computer code (refs. 3 and 4). The fiberglass blade set was designed for use in the R-12 ("Freon-12") test environment of the TDT and has scaled aeroelastic properties in R-12 similar to those of a full-scale utility-class helicopter. The aluminum blade set was designed for Mach-number-scaled testing in air. Due to rotor speed limitations of the test-bed model, full-scale tip Mach number values were not possible for this test. Both blade sets have identical rectangular planforms, are untwisted, and use a NACA 0012 airfoil. Blade geometry for both sets is shown in figure 2. The solidity for both rotor configurations was 0.0982. The mass and inertial characteristics of the blades may be varied by altering the distributions of tungsten and aluminum weights located in two spanwise channels along each blade. Lock numbers of both blade sets were matched ($\gamma = 4.35$) by appropriate distributions of these ballast weights, thus eliminating track effects caused by variations in blade flapping inertia. The ballast weights do not alter the stiffness distributions of the blades.

The test-bed used for this experiment was the NASA/U.S. Army aeroelastic rotor experimental system (ARES) model, shown in figure 3. The ARES model has a streamlined fuselage shell that encloses the rotor controls and drive system. The fuselage shell is not usually installed when testing the ARES model in the HHF and was omitted during this test. The model rotor is powered by a variable-frequency synchronous electric motor (rated at 47 hp output at 12 000 rpm) that is connected to the rotor shaft through a belt-driven two-stage speed reduction system. Blade collective pitch inputs and lateral and longitudinal cyclic pitch inputs are provided through a conventional swashplate arrangement, with the swashplate positioned by three electrically controlled hydraulic actuators. Root pitch adjustments to individual blades are made using a motorized pitch link system. The rotor control system is remotely operated from the HHF control room, with instrumentation mounted on the ARES model providing a continuous display of model control settings, rotor forces and moments, blade loads, and pitch link loads. Rotary potentiometers mounted at the blade cuffs are used to measure flapping and lagging on two of the four blades. These potentiometer signals are transferred to the fixed system through a 30-channel slip-ring assembly. Rotor forces and moments are measured in the nonrotating system by a six-component strain-gauge balance mounted below the drive system.

Test Procedure

This test was designed to provide a direct comparison of the coning and tracking characteristics of the two blade configurations. Baseline data were obtained for each set of blades, with all blades tracked with respect to the reference blade. At each test condition the rotor speed was set to 650 rpm. Blade collective pitch was swept from 0° to 16°, with data being collected at every 1° increment. Repeat measurements were made from 16° collective pitch to 0° collective pitch in increments of 2°. The nominal tip Mach number was 0.27 for the entire test. Blade track was visually monitored by means of a stroboscopic light system. Subsequent runs were performed similarly with the blade opposite the reference blade forced out of track by providing an offset in the root pitch of that blade ($\Delta\theta = -2°, -1°, +1°, +2°$). At each test point 5 seconds of data were obtained (corresponding to approximately 54 rotor revolutions). Blade position data and rotor force and moment data were sampled at a rate of 1000 samples per second per channel, averaged, and stored digitally. Rotor thrust and torque were calculated from the balance normal force and yawing moment channels, with balance interactions removed during off-line data reduction.

Presentation of Results

Plots are presented in figures 4 and 5 of induced blade out-of-track ($\Delta\beta$) versus the ratio of thrust coefficient to solidity (C_T/σ) for each rotor configuration. Figure 6 is a comparison of blade out-of-track versus blade root pitch offset for both sets of blades at various fixed thrust levels. Coning response versus rotor thrust for the baseline in-track cases of each rotor are compared in figure 7.

Because of an error in setting the root pitch during one run, measurements at the desired $\Delta\theta$ of +2° were not made for the aluminum blades. The $\Delta\theta$ for the run shown is estimated to be approximately +1.5°. Repeatability for C_T/σ has been estimated to be within ±0.0025. Accuracy of the angular measurements is estimated to be within ±0.1°. Repeatability for the angular measurements is within ±0.05°.

Discussion of Results

The results presented in figures 4 and 5 show that both rotors exhibit essentially the same trends in induced blade out-of-track due to the incremental adjustments made in root pitch. Cross-plots of $\Delta\beta$

versus $\Delta\theta$ at fixed values of C_T/σ (fig. 6) indicate that the fiberglass blades are perhaps slightly less responsive to the root pitch inputs than the aluminum blades. It should be emphasized that the differences in sensitivity shown here are on the limits of the resolution of the data.

Figure 7 shows the in-track coning angle (β) versus the ratio of thrust coefficient to solidity (C_T/σ) for both configurations. These data show a slight but measurable difference in the coning behavior of the two rotor configurations at higher values of C_T/σ; specifically, the fiberglass spar blades exhibit less coning (approximately 0.2°) than the aluminum spar blades. This behavior could be the result of an effective nose-down twist caused by "propeller moment" (ref. 5) acting on the blades at the higher collective pitch settings. As the fiberglass blades are significantly less stiff in torsion than the aluminum blades, they presumedly would be more susceptible to propeller moment-induced twist.

Concluding Remarks

The sensitivity of blade tracking in hover to variations in root pitch was determined experimentally for two rotor configurations possessing large differences in flapping and torsional stiffnesses. The data obtained here indicate that both rotors exhibit, for the most part, a similar sensitivity to root pitch adjustment in hover. However, slight differences in coning response between the two configurations are observed at higher thrust levels. Although no analysis is presented in this paper, the experimental data shown here may eventually prove useful to the rotor blade designer in diagnosing or preventing some blade tracking difficulties, and to the analyst in validating future rotor aeroelastic theories.

NASA Langley Research Center
Hampton, VA 23665-5225
November 5, 1991

References

1. Mantay, Wayne R.; and Yeager, William T., Jr.: *Parametric Tip Effects for Conformable Rotor Applications.* NASA TM-85682, AVRADCOM TR-83-B-4, 1983.

2. Mantay, Wayne R.; and Yeager, William T., Jr.: *Aeroelastic Considerations for Torsionally Soft Rotors.* NASA TM-87687, USAAVSCOM TR-86-B-1, 1986.

3. Johnson, Wayne: *A Comprehensive Analytical Model of Rotorcraft Aerodynamics and Dynamics. Part I: Analysis Development.* NASA TM-81182, USAAVRADCOM TR-80-A-5, 1980.

4. Johnson, Wayne: *A Comprehensive Analytical Model of Rotorcraft Aerodynamics and Dynamics. Part II: User's Manual.* NASA TM-81183, USAAVSCOM TR-80-A-6, 1980.

5. Johnson, Wayne: *Helicopter Theory.* Princeton Univ. Press, c.1980.

Table I. Properties of Fiberglass Model Blade

(a) Structural properties

Inboard section, r/R	Section mass, slugs	Stiffness, lb-ft^2			I_θ, lb-sec^2
		Flap	Chord	Torsion	
0.055	5.11×10^{-2}	3.47×10^4	3.47×10^4	6.94×10^3	5.70×10^{-4}
.125	4.57×10^{-3}	3.47×10^3	1.04×10^4	3.47×10^3	1.14×10^{-4}
.161	2.22×10^{-3}	2.78×10^2	1.74×10^3	2.78×10^2	6.49×10^{-5}
.193	8.82×10^{-3}	2.69×10^2	1.86×10^3	3.04×10^2	1.46×10^{-4}
.227	1.31×10^{-2}	2.69×10^2	1.86×10^3	3.04×10^2	1.56×10^{-4}
.280	2.55×10^{-4}	1.73×10^2	1.75×10^3	2.36×10^2	8.41×10^{-5}
.284	3.48×10^{-3}	1.73×10^2	1.75×10^3	2.36×10^2	8.98×10^{-5}
.325	8.65×10^{-3}	1.60×10^2	2.11×10^3	1.63×10^2	8.68×10^{-5}
.432	6.43×10^{-3}	1.26×10^2	1.83×10^3	1.37×10^2	8.49×10^{-5}
.514	3.18×10^{-2}	1.05×10^2	1.70×10^3	1.17×10^2	8.35×10^{-5}
.927	2.45×10^{-3}	1.05×10^2	1.70×10^3	1.17×10^2	8.35×10^{-5}
.959	3.67×10^{-4}	1.11×10^2	1.70×10^3	1.22×10^2	8.52×10^{-5}
.964	2.45×10^{-3}	3.47×10^2	3.47×10^3	3.47×10^2	1.03×10^{-4}
.982	4.72×10^{-4}	2.81×10^2	2.78×10^3	2.78×10^2	9.23×10^{-5}
.986	2.57×10^{-4}	3.47×10^1	3.47×10^2	3.47×10^1	1.14×10^{-5}

(b) Blade rotating natural frequencies

Modal identity	$^*\omega/\Omega$
Flap	2.61
Chord	4.18
Flap	4.83
Torsion	15.61

$^*\Omega = 68.07$ rad/sec

Table II. Properties of Aluminum Model Blade

(a) Structural properties

Inboard section, r/R	Section mass, slugs	Stiffness, lb-ft^2			I_θ, lb-sec^2
		Flap	Chord	Torsion	
0.055	5.11×10^{-2}	3.47×10^{4}	3.47×10^{4}	6.94×10^{3}	5.70×10^{-4}
.125	4.57×10^{-3}	3.47×10^{3}	1.04×10^{4}	3.47×10^{3}	1.14×10^{-4}
.161	2.27×10^{-3}	1.01×10^{3}	9.38×10^{3}	1.39×10^{3}	4.70×10^{-5}
.193	8.59×10^{-3}	9.72×10^{2}	8.68×10^{3}	1.04×10^{3}	7.43×10^{-5}
.227	1.39×10^{-2}	9.72×10^{2}	8.68×10^{3}	1.04×10^{3}	1.15×10^{-4}
.280	3.27×10^{-4}	1.01×10^{3}	9.38×10^{3}	1.39×10^{3}	8.87×10^{-5}
.284	2.95×10^{-3}	8.47×10^{2}	8.68×10^{3}	1.15×10^{3}	7.95×10^{-5}
.325	4.67×10^{-3}	7.47×10^{2}	8.47×10^{3}	1.02×10^{3}	7.49×10^{-5}
.400	2.63×10^{-3}	7.47×10^{2}	8.47×10^{3}	1.02×10^{3}	9.84×10^{-5}
.432	6.37×10^{-3}	6.20×10^{2}	8.33×10^{3}	7.76×10^{2}	9.38×10^{-5}
.514	2.98×10^{-2}	5.22×10^{2}	7.92×10^{3}	6.47×10^{2}	9.06×10^{-5}
.918	8.61×10^{-4}	5.22×10^{2}	7.92×10^{3}	6.47×10^{2}	1.17×10^{-4}
.927	3.13×10^{-3}	5.22×10^{2}	7.92×10^{3}	6.47×10^{2}	1.17×10^{-4}
.959	4.72×10^{-4}	6.25×10^{2}	8.33×10^{3}	6.94×10^{2}	1.21×10^{-4}
.964	2.62×10^{-3}	9.72×10^{2}	8.33×10^{3}	6.94×10^{2}	1.11×10^{-4}
.982	5.48×10^{-4}	8.33×10^{2}	7.64×10^{3}	6.25×10^{2}	9.23×10^{-5}
.986	2.56×10^{-4}	3.47×10^{1}	3.47×10^{2}	3.47×10^{1}	1.14×10^{-5}

(b) Blade rotating natural frequencies

Modal identity	$^*\omega/\Omega$
Flap	3.28
Flap	7.78
Chord	7.99
Torsion	15.50

$^*\Omega = 68.07$ rad/sec

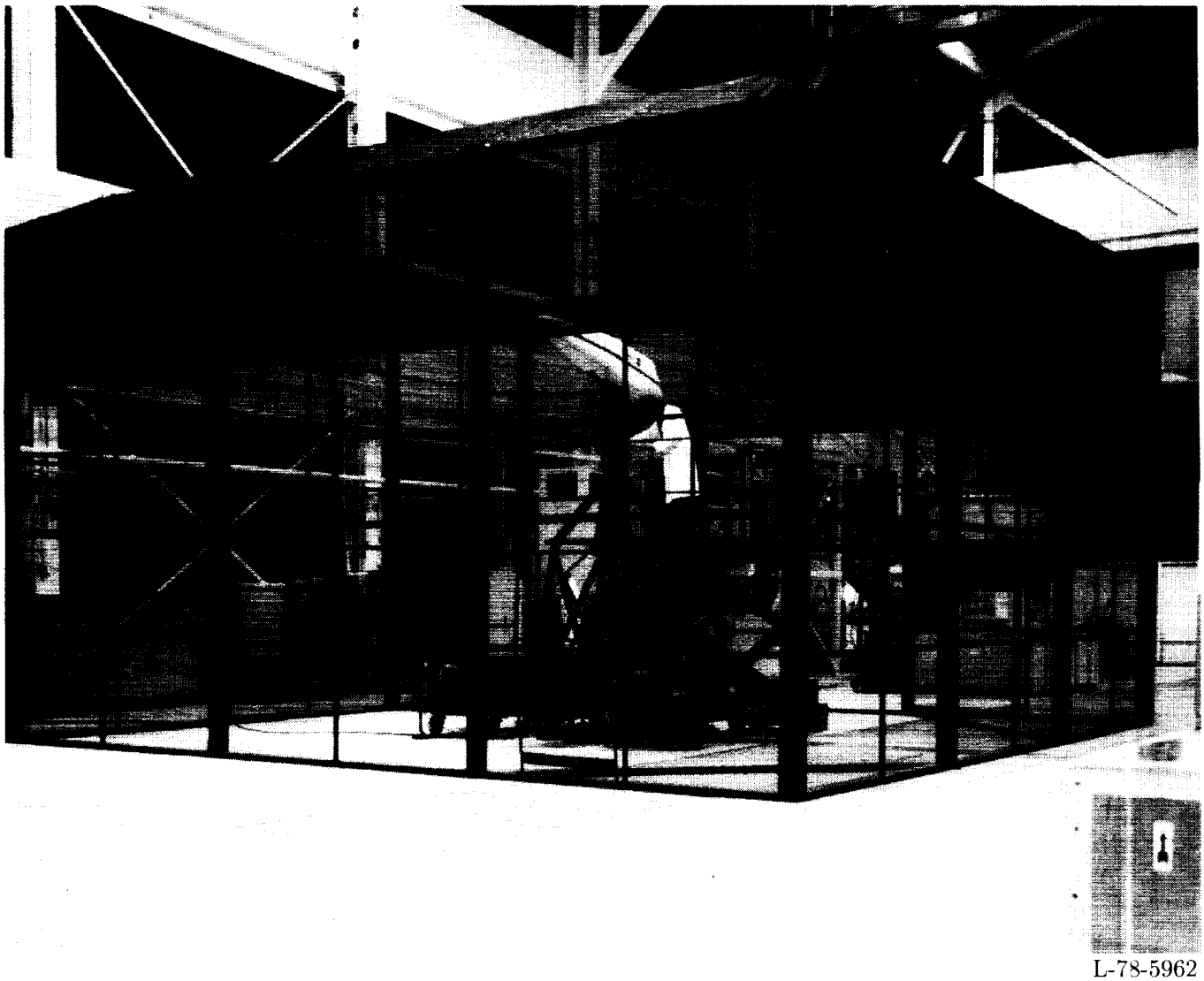

L-78-5962

Figure 1. Helicopter Hover Facility (HHF).

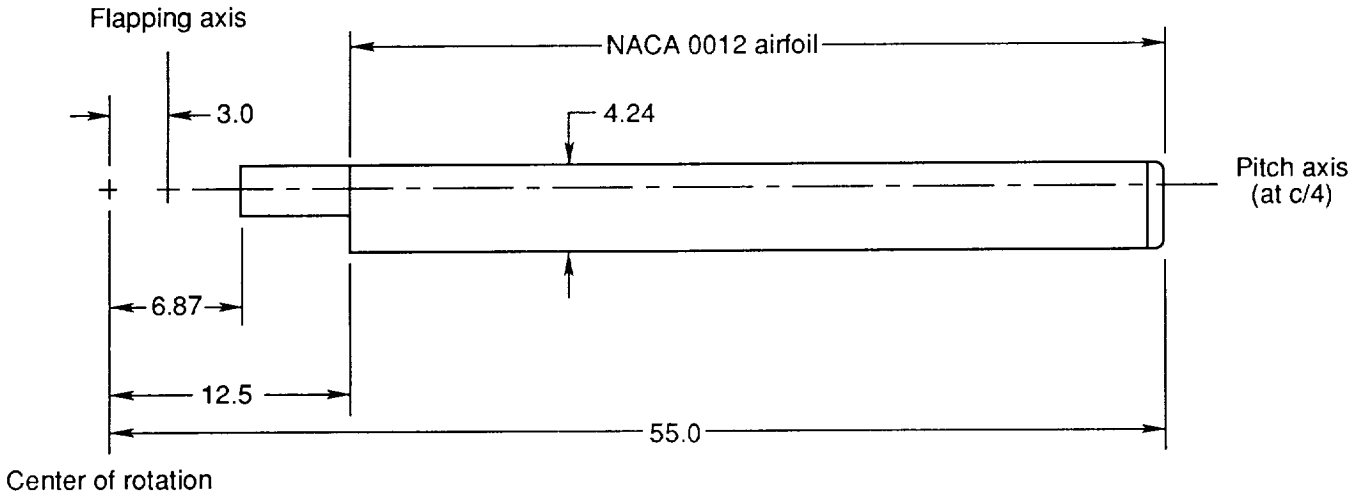

Figure 2. Rotor blade geometry. Dimensions in inches.

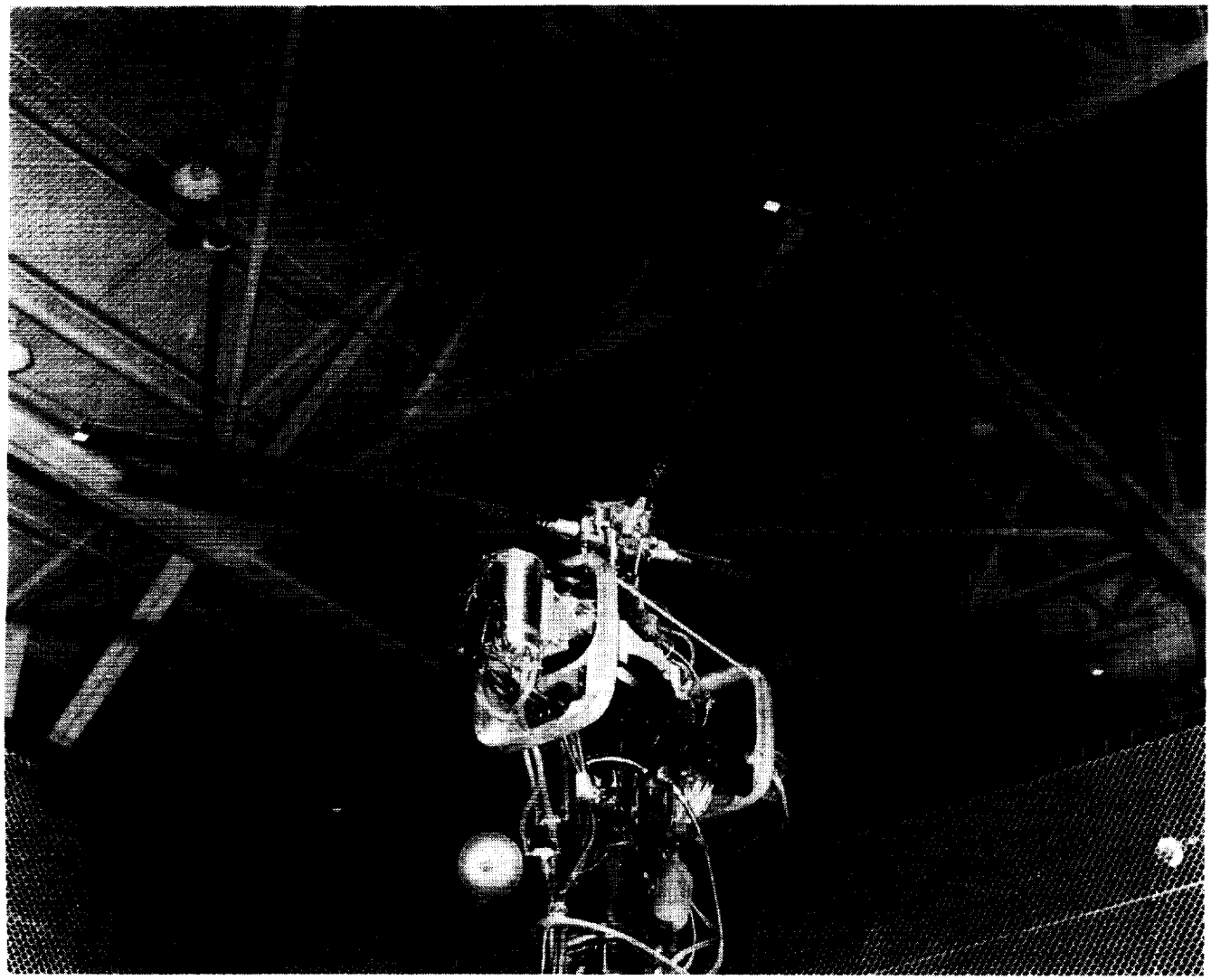

L-86-11,726

Figure 3. ARES model mounted in HHF.

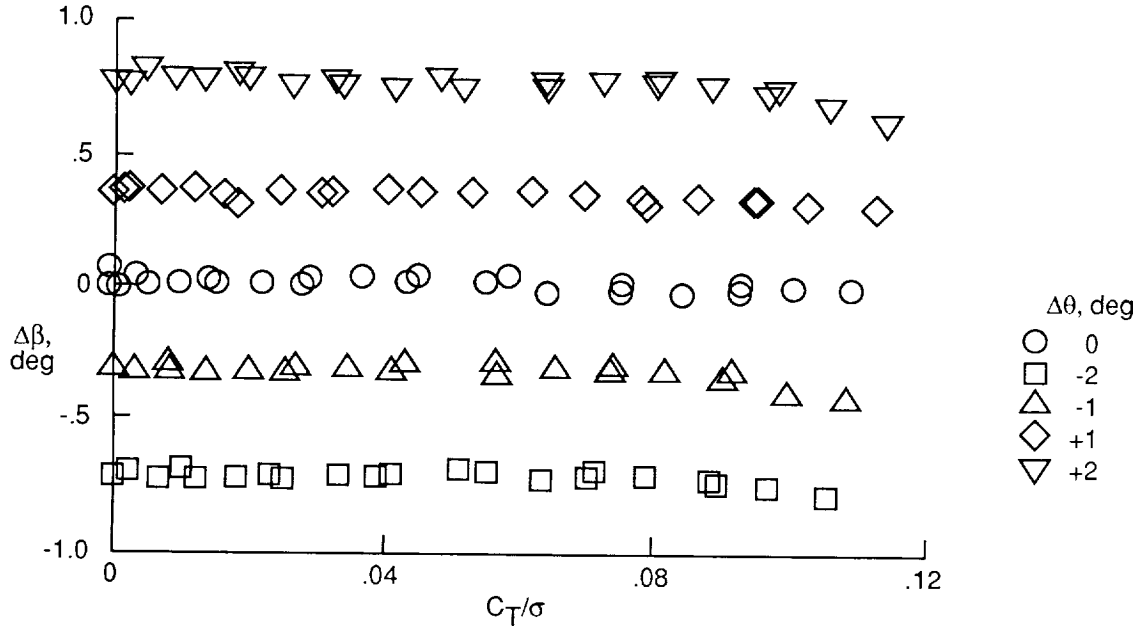

Figure 4. Tracking response to root pitch adjustment for fiberglass spar blades.

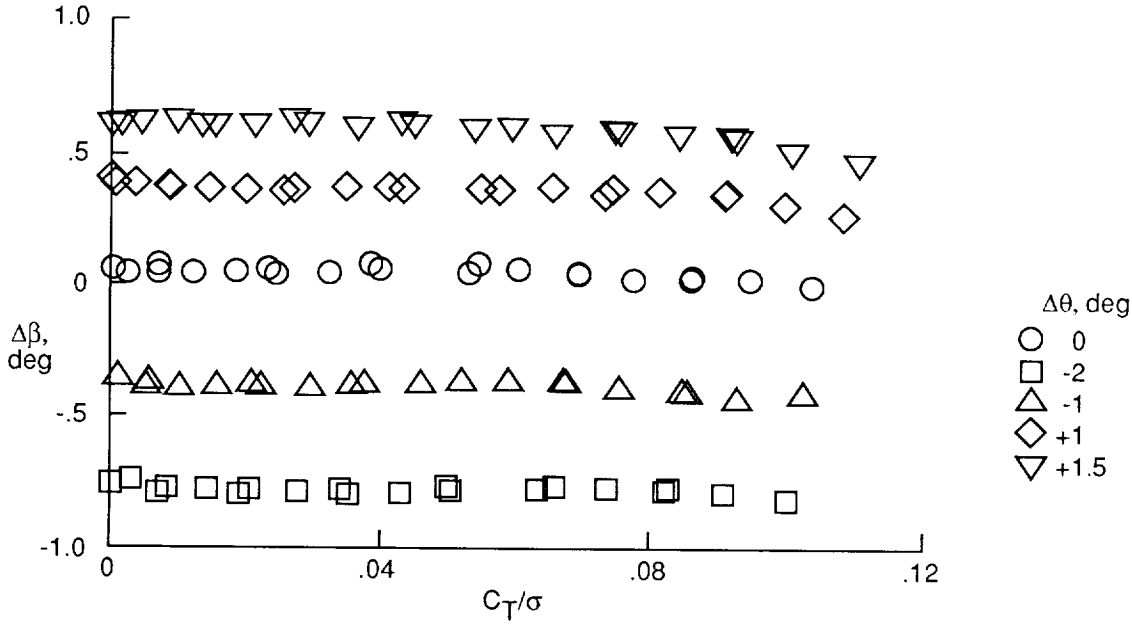

Figure 5. Tracking response to root pitch adjustment for aluminum spar blades.